RESEARCH LETTER

Transcriptional profiling of the marine oil-degrading bacterium *Alcanivorax borkumensis* during growth on *n*-alkanes

Julia S. Sabirova[1], Anke Becker[2], Heinrich Lünsdorf[3], Jean-Marc Nicaud[4], Kenneth N. Timmis[5] & Peter N. Golyshin[6]

[1]Department of Bioscience and Bioengineering, Ghent University, Ghent, Belgium; [2]Institute of Biology III, Faculty of Biology, University of Freiburg, Freiburg, Germany; [3]Department of Vaccinology and Applied Microbiology, HZI-Helmholtz Centre for Infection Research, Braunschweig, Germany; [4]Laboratoire de Microbiologie et de Génétique Moléculaire, INRA Centre de Grignon, Thiverval-Grignon, France; [5]Department of Environmental Microbiology, HZI-Helmholtz Centre for Infection Research, Braunschweig, Germany; and [6]School of Biological Sciences, Bangor University, Bangor Gwynedd, UK

Correspondence: Julia S. Sabirova, Laboratory of Industrial Microbiology and Biocatalysis, Faculty of Bioscience Engineering, Ghent University, Coupure Links 653, B-9000 Ghent, Belgium. Tel.: +32 9 264 93 85; fax: +32 9 264 62 31; e-mail: julia.sabirova@ugent.be

Received 21 December 2010; revised 15 March 2011; accepted 31 March 2011.
Final version published online 20 April 2011.

DOI:10.1111/j.1574-6968.2011.02279.x

Editor: Michael Galperin

Keywords
Alcanivorax borkumensis; alkane; transcriptomics.

Abstract

The marine oil-degrading bacterium *Alcanivorax borkumensis* SK2 has attracted significant interest due to its hydrocarbonoclastic lifestyle, its alkane-centered metabolism, and for playing an important ecological role in cleaning up marine oil spills. In this study, we used microarray technology to characterize the transcriptional responses of *A. borkumensis* to *n*-hexadecane exposure as opposed to pyruvate, which led to the identification of a total of 220 differentially expressed genes, with 109 genes being upregulated and 111 genes being downregulated. Among the genes upregulated on alkanes are systems predicted to be involved in the terminal oxidation of alkanes, biofilm formation, signal transduction, and regulation.

Introduction

Marine oil-degrading bacteria play an essential role in degrading crude oil and thus in cleaning up marine oil spills (Yakimov *et al.*, 2007). *Alcanivorax borkumensis* has become a paradigm of marine 'hydrocarbonoclastic' bacteria, as it exclusively grows on alkanes and plays a predominant ecological role in oil-degrading consortia that form following marine oil spills (McKew *et al.*, 2007; Gertler *et al.*, 2009). *Alcanivorax borkumensis* SK2 metabolizes a wide range of alkanes, such as linear alkanes, cyclo-alkanes, and isoprenoids (Dutta & Harayama, 2001; McKew *et al.*, 2007). Given its important ecological role in the removal of oil spills and with the availability of its full genome sequence (Schneiker *et al.*, 2006), *Alcanivorax* may now serve as a model organism to understand bacterial alkane metabolism.

Previous studies of bacterial alkane metabolism have been mostly focused on studying the terminal degradation of alkanes by *Pseudomonas putida* GPO1, a bacterium that uses linear alkanes as a single carbon and energy source, where a monooxygenase encoded by the *alkB1* gene plays a central role in the terminal oxidation of alkanes (van Beilen *et al.*, 1994). Other alkane-degrading bacteria use for this initial oxidation step enzymatic systems other than AlkB (for reviews, see van Beilen & Funhoff, 2007; Wentzel *et al.*, 2007). Our genome-wide study of alkane utilization by *A. borkumensis* using a proteomics approach has revealed several alternative systems for terminal oxidation of alkanes by this bacterium, as well as major rearrangements of its central carbon metabolism (Sabirova *et al.*, 2006). However, a number of specific questions intrinsically linked to alkane utilization by this organism, for example how alkanes enter the cell and which transport systems may be involved, how the cells physically interact with the hydrophobic substrate, whether and how they attach to it, and which molecular mechanisms allow the cells to protect themselves against the

toxic effect of alkanes, are left unanswered. Finally, the regulatory implications of alkane degradation on the overall cellular activity could not be comprehensively studied using the proteomic approach. To obtain a still more comprehensive picture of alkane utilization, and in particular to be able to look more closely into some of the aforementioned issues, we have now used microarray technology to compare the transcriptional profile of SK2 grown on *n*-hexadecane, as a model alkane, as compared with pyruvate, one of the few non-alkane substrates *A. borkumensis* is able to use.

Materials and methods

Bacterial strains and growth conditions

Alcanivorax borkumensis SK2 was used for all experiments. *Alcanivorax borkumensis* was grown until the late-exponential stage of growth as described earlier (Sabirova *et al.*, 2006). Bacteria from alkane- and pyruvate-grown cultures were centrifuged for 10 min at 8000 ***g***, and the cell pellets were immediately frozen in liquid nitrogen and conserved at $-80\,^{\circ}C$ until RNA was isolated.

Oligonucleotide design, printing, and layout of the *A. borkumensis* microarray

The Abo3kOLI microarray used in this study is based on the sequenced genome of *A. borkumensis* (Schneiker *et al.*, 2006). The array contains 2924 50mer to 70mer oligonucleotides representing predicted protein-encoding genes. In addition, the array contains 15 stringency controls of the genes *gap*, *rpsA*, *rpsO*, *rpsP*, and *rpmI* (70%, 80%, and 90% identity to the native sequence), 12 alien DNA oligonucleotides, and five spiking control oligonucleotides. Oligonucleotides were designed using OLIGODESIGNER software (Bioinformatics Resource Facility, CeBiTec, Bielefeld University). All oligonucleotide probes were printed in four replicates. Microarrays were produced and processed as described previously (Brune *et al.*, 2006). Oligonucleotides (40 μM) in 1.5 M betaine, 3 × SSC (1 × SSC is 0.15 M sodium chloride, 0.015 M sodium citrate) were printed onto Nexterion Slide E (Schott AG, Mainz, Germany) using the MicroGrid II 610 spotter (BioRobotics, Cambridge, UK) equipped with 48 SMP3 stealth pins (TeleChem International, Sunnyvale, CA). DNA was cross-linked to the surface by incubation of the slides for 2 h at 85 °C. Microarray data have been submitted to ArrayExpress under accession number A-MEXP-1990.

RNA isolation and synthesis of labeled cDNA

Total RNA was purified using the RNeasy Mini Kit (Qiagen, Hilden, Germany). Cells were disrupted in RLT buffer provided with the Kit in Fast Protein tubes (Qbiogene, Carlsbad, CA) using the Ribolyser (Hybaid, Heidelberg, Germany) (30 s, level 6.5) before spin column purification according to the RNeasy Mini Kit RNA purification protocol.

Fluorescent-labeled amplified RNA was prepared using the MessageAmp II-Bacteria RNA Amplification Kit (Applied Biosystems, Darmstadt, Germany). Starting from 500 ng total RNA, cDNA carrying a terminal T7 promoter was synthesized. Subsequent *in vitro* transcription resulted in aminoallyl-modified RNA that was labeled with Cy3- or Cy5-N-hydroxysuccinimidyl ester dyes (GE Healthcare, Little Chalfont, UK). Uncoupled dye was removed applying the RNeasy MinElute Kit (Qiagen).

Microarray hybridization and image acquisition

Processing of microarrays before hybridization included the following washes: once in 0.1% Triton-X100 (5 min, 20 °C); twice in 0.032% (w/v) HCl (2 min, 20 °C); once in 0.1 M KCl (10 min, 20 °C); once in H_2O (1 min, 20 °C); once in 0.064% (w/v) HCl, 1 × Nexterion blocking solution (Schott AG) (15 min, 50 °C); and once in H_2O (1 min, 20 °C). Microarrays were dried by centrifugation (3 min, 185 ***g***, 20 °C).

Hybridization was performed in an EasyHyb hybridization solution (Roche, Mannheim, Germany) supplemented with sonicated salmon sperm DNA at 50 μg mL^{-1} in a final volume of 100 μL for 90 min at 45 °C using the HS 4800 hybridization station (Tecan Trading AG, Switzerland). Before application to the microarrays, labeled samples were denatured for 5 min at 65 °C.

After hybridization microarrays were washed once in 2 × SSC, 0.2% sodium dodecyl sulfate (SDS) (w/v) (5 min, 42 °C), twice in 0.2 × SSC, 0.1% SDS (w/v) (1 min, 21 °C), twice in 0.2 × SSC (1 min, 21 °C), and once in 0.05 × SSC (1 min, 21 °C). Following the washes, slides were dried by centrifugation (3 min, 185 ***g***, 20 °C) and scanned with a pixel size of 10 μm using the LS Reloaded microarray scanner (Tecan Trading AG). Four independent biological replicates including a dye swap were processed for each comparison.

Transcriptome data analysis

The mean signal and the mean background intensities were obtained for each spot of the microarray images using the IMAGENE SOFTWARE 6.0 software (Biodiscovery Inc., Los Angeles) for spot detection, image segmentation, and signal quantification.

Spots were flagged as 'empty' if $R \leq 0.5$ in both channels, where $R = (\text{signal mean} - \text{background mean})/\text{background SD}$. The remaining spots were considered for further analysis. After subtractions of the local background intensities from the signal intensities and the introduction of a floor value of 20, the $\log_2$ value of the ratio of intensities was calculated for each spot using the formula $M_i = \log_2(R_i/G_i)$. $R_i = I_{ch1(i)} - Bg_{ch1(i)}$ and $G_i = I_{ch2(i)} - Bg_{ch2(i)}$, where $I_{ch1(i)}$

or $I_{ch2(i)}$ is the intensity of a spot in channel 1 or channel 2 and $Bg_{ch1(i)}$ or $Bg_{ch2(i)}$ is the background intensity of a spot in channel 1 or channel 2, respectively. The mean intensity was calculated for each spot, $A_i = \log_2(R_iG_i)^{0.5}$ (Dudoit *et al.*, 2002). A normalization method based on local regression was applied according to Yang *et al.* (2002), $M_i = \log_2(R_i/G_i) \rightarrow \log_2(R_i/G_i) - c(A) = \log_2(R_i/[k_j(A)G_i])$, where c(A) is the LOWESS (locally weighted scatter plot smoothing) fit to the MA plot.

Significant up- or downregulation of genes was identified by *t* statistics (Dudoit *et al.*, 2002). Genes were accounted as differentially expressed if $P \leq 0.05$ and $M \geq 1.00$ or ≤ -1.00.

Normalization and *t* statistics were carried out using the EMMA 2.2 microarray data analysis software developed at the Bioinformatics Resource Facility, Center for Biotechnology, Bielefeld University (Dondrup *et al.*, 2003).

Electron microscopy

For scanning electron microscopy (SEM), cells were grown on Permanox slides in ONR7a with either 1.5% hexadecane or 2% pyruvate as the carbon/energy source. SEM was carried out as described by Lünsdorf *et al.* (2001).

Results and discussion

The microarray experiments were performed with the exponentially grown cells grown on either hexadecane or pyruvate (as control conditions), and led to the identification of a total of 220 differentially expressed genes, with 109 genes being upregulated and 111 genes being downregulated. Differentially expressed genes could be grouped into 15 functional categories, according to designated metabolic functions of the corresponding gene products. Both upregulated and downregulated genes were found in most groups, with the exception of those genes grouped under 'alkane oxidation', 'stress', and 'iron uptake', whose functions were exclusively induced in the presence of alkanes. 'Nitrogen assimilation' genes were all found to be expressed on pyruvate only, as were a number of other genes known to enable the cells to assimilate essential macroelements other than N, namely phosphorus and sulfur from less favorable sources. This effect may at least partially be attributed to higher cell densities present in pyruvate cultures, leading to some scarcity of these macroelements in the pyruvate, but not yet in the alkane-grown cultures. In the following, we therefore focus primarily on the functions that were found to be upregulated on alkanes, and thus can most clearly be attributed to *A. borkumensis* responses to growth on alkanes.

Terminal oxidation of alkanes

The presence of an enzymatic system mediating the terminal oxidation of alkanes distinguishes an alkane-degrader from a non-alkane-degrading organism. Our earlier proteomic study has already revealed the presence of several alternative ways for the terminal oxidation of alkanes by *A. borkumensis* (Sabirova *et al.*, 2006). In accordance with the proteomic data, here, we find alkane monooxygenase *alkB1* (ABO_2707, Table 1) to be upregulated on hexadecane. Moreover, a second alkane monooxygenase *alkB2* (ABO_0122, Table 1) was also found to be upregulated, which corresponds to data using earlier reverse transcriptase-PCR (Schneiker *et al.*, 2006). In addition, two flavin-binding monooxygenases were found to be upregulated during growth on alkanes indicative of two novel pathways likely to be involved in alkane degradation by *A. borkumensis* (ABO_0282, ABO_1097, Table 1). Moreover, we detected the up-expression of two genes similar to the ones involved in the degradation of halogenated alkanes in other bacteria, namely haloacid dehalogenase-like hydrolase *dhlA* (ABO_1537, Table 1) and haloalkane dehalogenase *dhmA* (ABO_2415, Table 1). If the first enzyme is known to convert haloalkanes to corresponding alcohols and halides, the second one catalyzes hydrolytic cleavage of carbon-halogen bonds in halogenated aliphatic compounds, leading to the formation of primary alcohols, halide ions, and protons. Alkane-induced coexpression of these enzymes mediating the breakdown of haloalkanes, alongside the induction of enzymes degrading aliphatic alkanes, signifies unspecific upregulation of expression, probably reflecting the presence of halogenated alkanes in sea water. Additionally, we found alkane-induced expression of aldehyde reductase (ABO_2414, Table 1). This gene is predicted to be involved in the metabolic activation of polycyclic aromatic hydrocarbons (PAHs), as shown recently for human aldehyde reductase *AKR1A1* (Palackal *et al.*, 2001). However, as yet, *A. borkumensis* has not been shown to either degrade or transform PAHs, and thus requires further experimentation to explore what coexpression of this gene alongside those mediating the degradation of aliphatic alkanes may signify for the degradation of alkanes or petroleum. These data allow us to update the list of enzymatic systems shown before by our proteomic study to be potentially involved in the initial terminal oxidation of alkanes by *A. borkumensis* (Figs 1 and 2).

Alkane-induced biofilm formation and adhesion to hydrocarbons

Attachment of *A. borkumensis* to hydrocarbons and its molecular mechanisms have not yet been studied, although such abilities are likely to form part of the specific ecological adaptation of this bacterium. EM observation of *Alcanivorax* SK2 indeed indicates that this organism forms biofilm-supporting structures during growth on alkanes (Fig. 3). Cells grown on alkane seem to more connect to each other rather than to the solid surface of the carrier slide, and they are shorter and rounder, and produce considerable amount

Table 1. Differentially expressed genes with known functions

Gene number*	Gene function or functional category*	ER	SD	Gene number*	Gene function or functional category*	ER	SD
Terminal oxidation of alkanes							
ABO_0122	Alkane-2-monooxygenase, AlkB2	+12.86	±0.40	ABO_0145	Ferredoxin – NADP+reductase, Frp	+10.14	±0.57
ABO_0282	Monooxygenase, flavin-binding family	+15.32	±0.30	ABO_1097	Monooxygenase, flavin-binding family	+7.81	±0.72
ABO_1537	Haloacid dehalogenase-like hydrolase, DhlB	+18.75	±0.28	ABO_1717	Flavodoxin reductase	+8.51	±0.55
ABO_2107	Monooxygenase, putative	+4.77	±0.88	ABO_2414	Aldehyde reductase, AKR1A1	+14.02	±0.41
ABO_2415	Haloalkane dehalogenase, DhmA	+12.52	±0.40	ABO_2483	Alcohol dehydrogenase	+6.39	±0.64
ABO_2707	Alkane 1-monooxygenase, AlkB1	+6.67	±0.72	ABO_2845	Ferredoxin, 2Fe-2S	+6.48	±0.67
Energy and carbon metabolism							
ABO_0543	Respiratory nitrate reductase 1 gamma chain, NarI	+3.66	±1.79	ABO_1753	3-dimethylubiquinone-9 3-O-methyltransferase, UbiG	+3.34	±1.26
ABO_2036	Cytochrome c oxidase, subunit I, CyoB	+5.75	±0.79	ABO_1238	Enoyl-CoA hydratase/isomerase, putative	+4.79	±0.89
ABO_1652	Fatty oxidation complex, FadB2	+11.01	±0.46	ABO_1653	3-oxoacyl-CoA thiolase, FadA2	+9.20	±0.60
ABO_1701	Acyl-CoA dehydrogenase, C-terminal domain, AcdA	+5.83	±0.87	ABO_2102	Acyl-CoA dehydrogenase, putative	+9.03	±0.59
ABO_1445	Sugar aldolase, putative	+5.11	±0.86	ABO_2741	Isocitrate lyase	+23.17	±0.20
ABO_0211	Phosphoglucomutase/phosphomannomutase	−4.37	±0.93	ABO_0426	Glycerophosphoryl diester phosphodiesterase precursor	−5.95	±0.79
ABO_1042	Glycerophosphoryl diester phosphodiesterase, putative	−8.07	±0.52	ABO_2613	Phosphoglycerate kinase, pgk	−4.38	±0.90
ABO_2701	2′,3′-cyclic-nucleotide 2′-phosphodiesterase, CpdB	−3.67	±1.15	ABO_0840	Adenylate kinase, Adk	−8.47	±0.50
ABO_0885	Adenylate cyclase	−6.40	±0.69				
Stress-related genes							
ABO_2633	DNA-binding stress protein	+3.95	±1.22	ABO_0314	Heat shock protein, DnaK	+11.32	±0.39
ABO_0315	Heat shock protein, DnaJ	+14.67	±0.34	ABO_0633	Chaperonin, 10 kDa, GroES	+9.17	±0.51
ABO_0634	GroEL chaperonin, Cpn60	+17.84	±0.30	ABO_1180	Heat shock protein, HtpX	+11.67	±0.54
ABO_1489	Heat shock protein, HtpG	+13.37	±0.42	ABO_1777	Heat-shock protein, IbpA	+17.45	±0.27
ABO_2244	Heat shock protein, HslV	+11.67	±0.49	ABO_2245	Heat shock protein, HslU	+9.72	±0.51
ABO_0095	Lactoylglutathione lyase, GloA	+10.22	±0.56	ABO_0649	Superoxide dismutase, SodB	+9.99	±0.40
ABO_1531	Protein-methionine-*S*-oxide reductase, MsrB	+7.05	±0.70	ABO_2703	Peptide methionine sulfoxide reductase, MsrA	+3.81	±1.13
ABO_0758	TolB protein	+6.86	±0.65				
Transport systems							
ABO_2119	Flavohemoprotein, HmpA	+13.29	±0.41	ABO_2370	Fe3+-hydroxamate ABC transporter protein	+6.60	±0.61
ABO_2487	Ferripyoverdine receptor precursor, FpvB	+6.97	±1.14	ABO_1360	Copper-translocating P-type ATPase	+13.64	±0.34
ABO_1364	Copper-binding protein, CopC	+9.83	±0.57	ABO_1411	OmpA family protein	+11.81	±0.46
ABO_0618	Sodium/alanine symporter, Dag A	−6.71	±0.61	ABO_0851	Nitrate transport ATP-binding protein, NtrC	−3.40	±2.93
ABO_0852	Nitrate ABC transporter permease protein, NtrB	−3.93	±1.07	ABO_1668	Ion transport protein	−4.61	±0.93
ABO_1888	Sulfonate ABC transporter protein	−5.45	±0.75	ABO_2509	Branched-chain amino acid ABC transporter	−3.88	±1.23
ABO_2512	Branched-chain amino acid ABC transporter, ATP-binding protein, putative	−6.40	±0.89	ABO_2513	Amino acid ABC transporter, ATP-binding protein	−5.35	±0.92

Table 1. Continued.

Gene number*	Gene function or functional category*	ER	SD	Gene number*	Gene function or functional category*	ER	SD
ABO_2544	Small multidrug resistance protein	−9.19	±0.48	ABO_2684	Phosphate ABC transporter permease protein	−6.81	±0.85
Cell wall metabolism							
ABO_0601	Cell division protein, FtsQ	+3.84	±1.28	ABO_0603	Cell division protein, FtsZ	+10.02	±0.45
ABO_0120	Amidase, AmiC	+6.19	±0.73	ABO_1957	Membrane-bound lytic murein transglycosylase B	+4.60	±0.90
ABO_0260	Effector of murein hydrolase, putative	−4.00	±1.12	ABO_1221	Membrane-bound lytic murein transglycosylase D	−7.82	±0.58
ABO_1425	Soluble lytic transglycosylase, putative	−11.06	±0.39	ABO_2215	Heptosyltransferase II, putative	−11.43	±0.54
Biofilm, formation of alginate							
ABO_0395	Mannose-6-phosphate isomerase, AlgA	+12.31	±0.48	ABO_0126	Type-1 fimbrial protein, A chain precursor	+15.45	±0.39
ABO_0584	Phosphoheptose isomerase, GmhA	+6.63	±0.62	ABO_0463	Pilus biogenesis protein, PilN	−6.59	±0.62
ABO_0467	Pilin biogenesis-related protein	−10.02	±0.40	ABO_0613	Type IV pilus assembly protein, TapC	−10.74	±0.53
ABO_0614	IV fimbrial assembly protein, PilB	−6.14	±0.74	ABO_2670	IV pili twitching motility protein, PilT	−5.19	±0.78
Transcriptional regulators							
ABO_0031	Transcriptional regulatory protein, Qseb	+7.52	±0.60	ABO_0121	Transcriptional regulator, GntR family	+9.19	±0.48
ABO_1680	DnaK suppressor protein homolog, DksA1	+4.37	±0.93	ABO_1708	Sensor histidine kinase	+11.58	±0.38
ABO_1709	DNA-binding response regulator	+10.82	±0.38	ABO_2132	HD-GYP domain protein	+3.79	±1.26
ABO_0005	DNA-binding protein H-NS	−5.36	±0.76	ABO_0104	Two-component hybrid chemotactic sensor and regulator, ChpA, putative	−7.52	±0.94
ABO_0167	Phosphate regulon sensor protein, PhoR	−7.48	±0.64	ABO_0428	DNA-binding response regulator, LuxR family	−11.76	±0.35
ABO_0472	Two-component sensor histidine kinase, PilS	−8.24	±0.49	ABO_0859	Nitrogen assimilation response regulatory protein	−7.40	±0.63
ABO_1745	Stringency control	−6.78	±0.65	ABO_1840	Stringency control	−11.76	±0.34
ABO_1986	Two-component sensor histidine kinase protein, putative	−7.13	±1.02	ABO_2018	Sensor histidine kinase/response regulator	−10.05	±0.53
ABO_2023	Catabolite gene activator, Crp	−9.52	±0.52	ABO_2260	Sensory box histidine kinase, NtrB	−6.55	±0.61
ABO_2433	Conserved hypothetical signal transduction protein	−7.14	±0.55	ABO_2508	Transcriptional regulator, GntR family	−16.05	±0.35
ABO_2519	Response regulator	−11.50	±0.37	ABO_2520	Sensor histidine kinase	−13.98	±0.29
ABO_2530	Nitrogen regulatory protein P-II, GlnK2	−7.49	±0.56	ABO_2581	Transcription regulator family protein, AcrR	−8.39	±0.51

*Gene numbers, gene function, and functional category are presented according to the annotated genome (Schneiker *et al.*, 2006).
ER, expression ratio; SD, standard deviation.

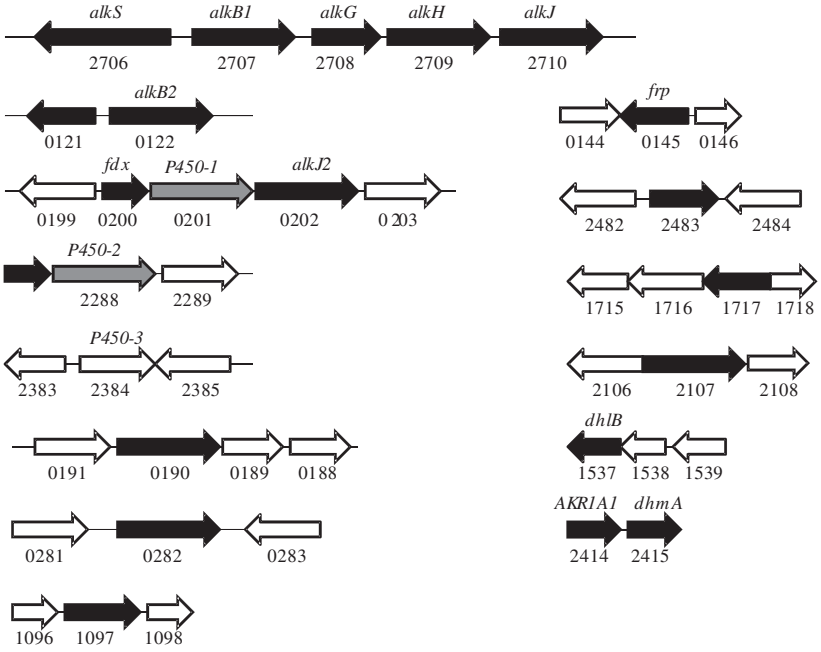

Fig. 1. Combined schematic representation of genomic regions containing genes encoding monooxygenases and enzymes presumably involved in the initial oxidation of alkanes derived from the analysis of proteomic (Sabirova *et al.*, 2006) and transcriptomic data. Genes upregulated in alkane-grown cells are shown in black; white-colored ORFs with black frames show genes in the *Alcanivorax borkumensis* genome that seem not to be upregulated; grey-colored ORFs show the P450-1 and P450-2 genes (ABO_0201 and ABO_2288, correspondingly), encoding identical p450 cytochrome proteins.

of extracellular polymeric substances (EPS), which appears to support the three-dimensional structure of a biofilm. After 10 days of growth, alkane-grown cells develop a biofilm, which exhibits a pronounced three-dimensional architecture supported by extracellular matrix (Fig. 3).

The argument of an alkane-induced formation of EPS is supported by alkane-induced up-expression of *gmhA* (ABO_0584). *GmhA* encodes a phosphoheptose isomerases that mediates the synthesis of heptose, a conserved component of outer membrane lipopolysaccharide, that for example in *Yersinia*, was shown to contribute to the formation of biofilms (Darby *et al.*, 2005). Another indication for alkane-induced biosynthesis of EPS in *Alcanivorax* could be the upregulation of mannose-6-phosphate isomerase *algA*, encoded by ABO_0395 (Table 1), predicted to encode an enzyme known to catalyze the first and third steps of the biosynthetic pathway of alginate, a known component of biofilms in other organisms (Shinabarger *et al.*, 1991); however, *algA*, like other related *alg* genes, may also be involved in the biosynthesis of lipopolysaccharide, as shown elsewhere (Goldberg *et al.*, 1993; Gaona *et al.*, 2004). As direct experimental evidence is still missing as regards alginate production by *Alcanivorax*, our findings may point more to the biosynthesis of lipopolysaccharide, rather than of alginate. While the biosynthesis of alginate has not yet been shown for *Alcanivorax*, it has been described for marine algae and bacteria belonging to the genera *Pseudomonas* and *Azotobacter* (Gorin & Spencer, 1966; Lin & Hassid, 1966; Evans & Linker, 1973).

With respect to the expression of genes thought to be involved in the signalling and regulatory processes essential for the formation of biofilm, our transcriptomic data show that the widely suggested mechanism of biofilm formation mediated by elevated concentrations of messenger c-di-GMP does not seem to be clearly effective in the case of *Alcanivorax* growing on alkanes. One regulatory system (encoded by ABO_2433), containing the known GGDEF and EAL domains, responsible for the biosynthesis and hydrolysis of c-di-GMP, respectively, was found to be downregulated, while another gene, ABO_2132 encoding the HD-GYP domain with phosphodiesterase activity responsible for hydrolysis of c-di-GMP (Galperin *et al.*, 1999; Ryan *et al.*, 2006), was found to be upregulated. Hence, the precise role of intracellular c-di-GMP levels for biofilm formation may be more complex than previously assumed (Hickman *et al.*, 2005; Römling *et al.*, 2005). We furthermore found that a whole set of genes involved in the formation of pili (ABO_0463, ABO_0467, ABO_0613, ABO_00614, and ABO_2670, Table 1) is downregulated during growth on alkanes; hence, attachment of *Alcanivorax* to alkane droplets does seem to require quorum sensing, and leads to enhanced biosynthesis of EPS, and yet, it may not be classical biofilms that are formed to access alkane droplets, triggered by intracellular c-di-GMP and by the formation of pili and/or fimbriae, but rather irregular aggregates glued together by extracellular polysaccharides.

Transport systems

Our expression data also shed some new light on the acknowledged uncertainty as to how alkanes are transported into the bacterial cell. One of the alkane-induced genes,

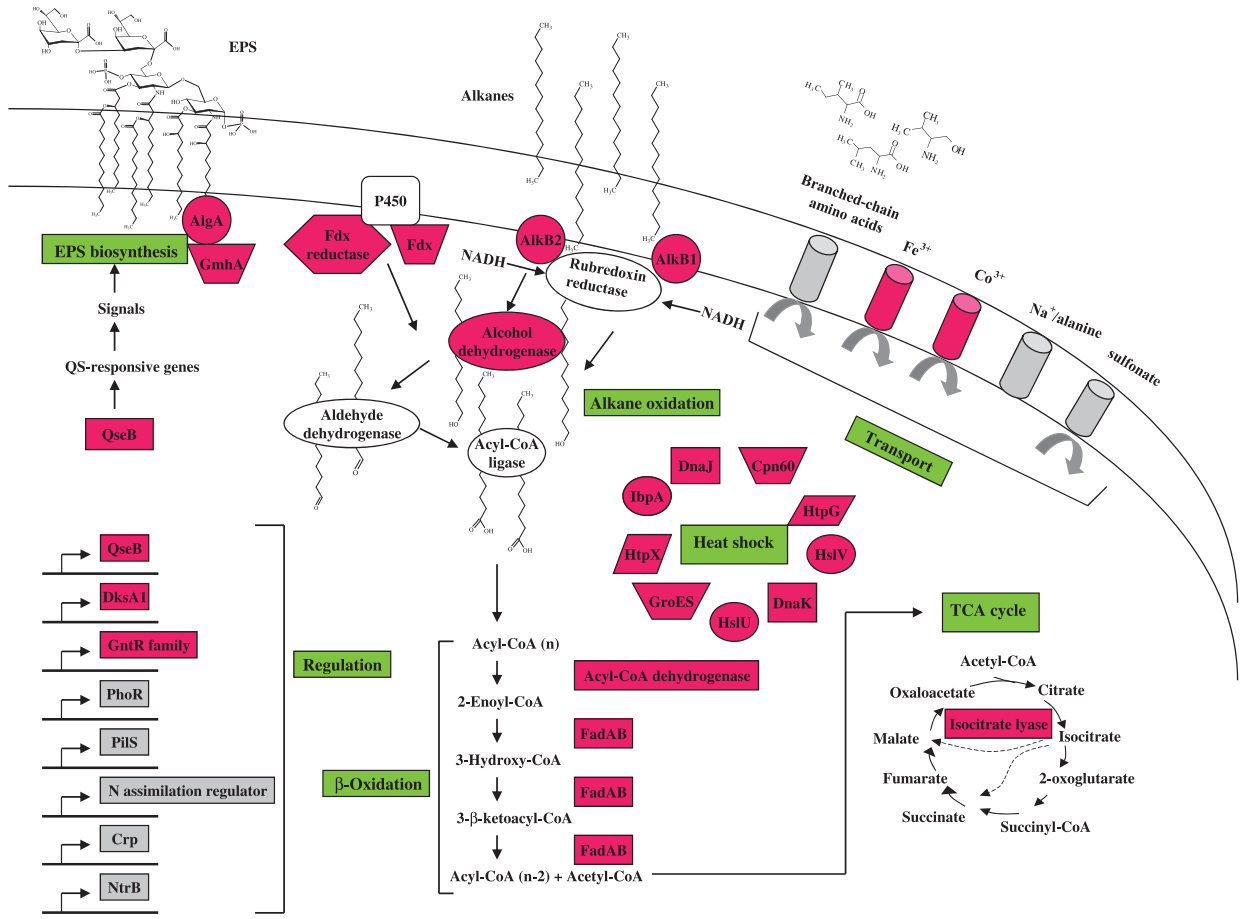

Fig. 2. Representation of the metabolic response of *Alcanivorax borkumensis* SK2 to alkane exposure as opposed to pyruvate. Genes repressed or induced after exposure to alkanes are shown with a grey or a red background, respectively.

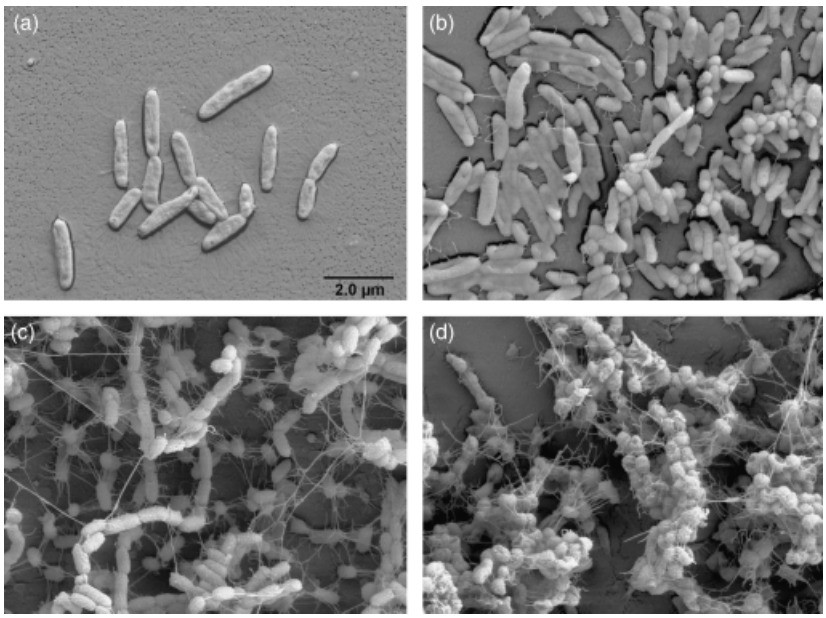

Fig. 3. Transmission electron microscopy observations of *Alcanivorax borkumensis* SK2 cells, their adhesion, and biofilm formation on abiotic surfaces. The cells were grown on either pyruvate (a, b) or hexadecane (c, d) on Permanox slides in ONR7a medium. The biofilms were monitored after 4 days (a, c) and 10 days (b, d) of growth.

ABO_0902 (see Supporting Information, Table S2), encoding an outer membrane lipoprotein Blc, may directly be involved in the alkane uptake process, as it contains a so-called lipocalin domain, which, in contact with organic solvents, forms a small hydrophobic pocket catalyzing the transport of small hydrophobic molecules, such as lipids and steroid hormones (Pervaiz & Brew, 1987). This alkane-induced protein would thus be a prime candidate potentially mediating alkane transport.

Regulation

Using a transcriptomics approach, a number of additional alkane-induced regulatory systems have been detected (Table 1), as compared with our previous proteomics study (Sabirova *et al.*, 2006). A transcriptional regulator of the GntR family, encoded by ABO_0121, is located next to the ABO_0122 encoding the *alkB2* monooxygenase, suggesting that the ABO_0121-encoded gene product might regulate the expression of the adjacent monooxygenase. Another regulatory system consisting of ABO_1708 and ABO_1709, adjacent to each other and likely to be operon-arranged, encodes a pair of sensor histidine kinase and DNA-binding response regulator that are also upregulated on alkanes. Their close proximity to the gene of fatty acid degradation (fadH dienoyl-CoA reductase) may indicate that this regulatory system controls the oxidation of fatty acids in *Alcanivorax*. Our transcriptome data also hint towards quorum sensing playing a role in biofilm formation of *Alcanivorax* on alkanes, as the major transcriptional regulator QseB encoded by ABO_0031 was found to be upregulated on hexadecane (Table 1). Quorum sensing has indeed been reported to trigger biofilm formation via the biosynthesis of extracellular exopolysaccharides (EPS) (Sauer *et al.*, 2002), also visible on our EM pictures. We did not detect increased expression of the cognate histidine kinase, QseC, encoded by ABO_0030. This finding indicates that for initial signal reception and transduction constant levels of sensor protein suffice, while the subsequent coordinated regulation of the expanded quorum-sensing regulon qse does require increased titers of Qse regulator protein. Finally, an HD-GYP domain protein encoded by ABO_2132 and mentioned earlier in 'Alkane-induced biofilm formation and adhesion to hydrocarbons' is also upregulated on alkanes and hence represents another worthy target for regulatory studies of growth on alkanes.

To conclude, our transcriptomics analysis of *A. borkumensis* responses to alkane exposure adds a complementary view on alkane metabolism by this bacterium, in addition to our previous proteomics study, and reveals a number of novel observations, for instance concerning the molecular mechanisms of alkane transport across the cytoplasmic membrane, and pointing to a diverse set of enzymes for the degradation of alkanes. *Alcanivorax* SK2 seems to respond to growth on alkanes by forming cell aggregates, probably supported by enhanced synthesis of EPS and probably following in a quorum-sensing-mediated aggregation process. Finally, the study has also revealed many transcriptional regulators to be differentially expressed, indicating a complex regulatory interplay of alkane degradation with other metabolic functions in this marine organism. Knocking out these alkane-responsive regulators should provide a valuable insight into the scope of regulons and subregulons essential for alkane degradation by *A. borkumensis* SK2.

Acknowledgements

This research was supported by a grant from the German Ministry for Education and Research (BMBF) in the frame of the GenoMik network 'Genome Research on Bacteria Relevant for Agriculture, Environment and Biotechnology' and by a short-term fellowship from the European Molecular Biology Organization (EMBO) (ASTF 354-2006).

References

Brune I, Becker A, Paarmann D, Albersmeier A, Kalinowski J, Pühler A & Tauch A (2006) Under the influence of the active deodorant ingredient 4-hydroxy-3-methoxybenzyl alcohol, the skin bacterium *Corynebacterium jeikeium* moderately responds with differential gene expression. *J Biotechnol* **127**: 21–33.

Darby C, Ananth SL, Tan L & Hinnebusch BJ (2005) Identification of *gmhA*, a *Yersinia pestis* gene required for flea blockage, by using a *Caenorhabditis elegans* biofilm system. *Infect Immun* **73**: 7236–7242.

Dondrup M, Goesmann A, Bartels D, Kalinowski J, Krause L, Linke B, Rupp O, Sczyrba A, Pühler A & Meyer F (2003) EMMA: a platform for consistent storage and efficient analysis of microarray data. *J Biotechnol* **106**: 135–146.

Dudoit S, Yang YH, Callow MJ & Speed TP (2002) Statistical methods for identifying differentially expressed genes in replicated cDNA microarray experiments. *Stat Sinica* **12**: 111–139.

Dutta TK & Harayama S (2001) Biodegradation of n-alkylcycloalkanes and n-alkylbenzenes via new pathways in *Alcanivorax* sp. strain MBIC 4326. *Appl Environ Microb* **67**: 1970–1974.

Evans LR & Linker A (1973) Production and characterization of the slime polysaccharide of *Pseudomonas aeruginosa*. *J Bacteriol* **116**: 915–924.

Galperin MY, Natale DA, Aravind L & Koonin EV (1999) A specialized version of the HD hydrolase domain implicated in signal transduction. *J Mol Microb Biotech* **1**: 303–305.

Gaona G, Núñez C, Goldberg JB, Linford AS, Nájera R, Castañeda M, Guzmán J, Espín G & Soberón-Chávez G (2004) Characterization of the *Azotobacter vinelandii algC* gene

involved in alginate and lipopolysaccharide production. *FEMS Microbiol Lett* **238**: 199–206.

Gertler C, Gerdts G, Timmis KN, Yakimov MM & Golyshin PN (2009) Populations of heavy fuel oil-degrading marine microbial community in presence of oil sorbent materials. *J Appl Microbiol* **107**: 590–605.

Goldberg JB, Hatano K & Pier GB (1993) Synthesis of lipopolysaccharide-O-side-chains by *Pseudomonas aeruginosa* PAO1 requires the enzyme phosphomannomutase. *J Bacteriol* **175**: 1605–1611.

Gorin PA & Spencer JF (1966) Exocellular alginic acid from *Azotobacter vinelandii*. *Can J Chem* **44**: 993–998.

Hickman JW, Tifrea DF & Harwood CS (2005) A chemosensory system that regulates biofilm through modulation of cyclic diguanylate levels. *P Natl Acad Sci USA* **102**: 14422–14427.

Lin TY & Hassid WZ (1966) Pathway of alginic acid synthesis in the marine brown alga, *Fucus gardneri* Silva. *J Biol Chem* **24**: 5284–5297.

Lünsdorf H, Strompl C, Osborn AM, Bennasar A, Moore ER, Abraham WR & Timmis KN (2001) Approach to analyse interactions of microorganisms, hydrophobic substrates and soil colloids leading to formation of composite biofilms, and to study initial events in microbiogeological processes. *Method Enzymol* **336**: 317–331.

McKew BA, Coulon F, Yakimov MM, Denaro R, Genovese M, Smith CJ, Osborn AM, Timmis KN & McGenity TJ (2007) Efficacy of intervention strategies for bioremediation of crude oil in marine systems and effects on indigenous hydrocarbonoclastic bacteria. *Environ Microbiol* **9**: 1562–1571.

Palackal NT, Burczynski ME, Harvey RG & Pennig TM (2001) Metabolic activation of polycyclic aromatic hydrocarbon trans-dihydrodiols by ubiquitously expressed aldehyde reductase (AKR1A1). *Chem Biol Interact* **130–132**: 815–824.

Pervaiz S & Brew K (1987) Homology and structure-function correlations between alpha 1-acid glycoprotein and serum retinol-binding protein and its relatives. *FASEB J* **1**: 209–214.

Römling U, Gomelsky M & Galperin MY (2005) C-di-GMP: the dawning of a novel bacterial signalling system. *Mol Microbiol* **57**: 629–639.

Ryan RP, Fouhy Y, Lucey JF *et al.* (2006) Cell-cell signaling in *Xanthomonas campestris* involves an HD-GYP domain protein that functions in cyclic di-GMP turnover. *P Natl Acad Sci USA* **103**: 6712–6717.

Sabirova JS, Ferrer M, Regenhardt D, Timmis KN & Golyshin PN (2006) Proteomic insights into metabolic adaptations in *Alcanivorax borkumensis* induced by alkane utilization. *J Bacteriol* **188**: 3763–3773.

Sauer K, Camper A, Ehrlich G, Costerton J & Davies D (2002) *Pseudomonas aeruginosa* displays multiple phenotypes during development as a biofilm. *J Bacteriol* **184**: 1140–1154.

Schneiker S, Martins dos Santos VA, Bartels D *et al.* (2006) Genome sequence of the ubiquitous hydrocarbon-degrading marine bacterium *Alcanivorax borkumensis*. *Nat Biotechnol* **24**: 997–1004.

Shinabarger D, Berry A, May TB, Rothmel R, Fialho A & Chakrabarty AM (1991) Purification and characterization of phosphomannose isomerase-guanosine diphospho-D-mannose pyrophosphorylase – a bifunctional enzyme in the alginate biosynthetic pathway of *Pseudomonas aeruginosa*. *J Biol Chem* **29**: 2080–2088.

Van Beilen JB & Funhoff EG (2007) Alkane hydroxylases involved in microbial alkane degradation. *Appl Microbiol Biot* **74**: 13–21.

Van Beilen JB, Wubbolts MG & Witholt B (1994) Genetics of alkane oxidation by *Pseudomonas oleovorans*. *Biodegradation* **5**: 161–174.

Wentzel A, Ellingsen TE, Kotlar H-K, Zotchev SB & Throne-Holst M (2007) Bacterial metabolism of long-chain *n*-alkanes. *Appl Microbiol Biot* **76**: 1209–1221.

Yakimov MM, Timmis KN & Golyshin PN (2007) Obligate oil-degrading marine bacteria. *Curr Opin Biotech* **18**: 257–266.

Yang YH, Dudoit S, Luu P, Lin DM, Peng V, Ngai J & Speed TP (2002) Normalization for cDNA microarray data: a robust composite method addressing single and multiple slide systematic variation. *Nucleic Acids Res* **30**: e15.

Supporting information

Additional Supporting Information may be found in the online version of this article:

Table S1. Other cellular functions.
Table S2. Hypothetical proteins with predicted and unknown functions.

Please note: Wiley-Blackwell is not responsible for the content or functionality of any supporting materials supplied by the authors. Any queries (other than missing material) should be directed to the corresponding author for the article.